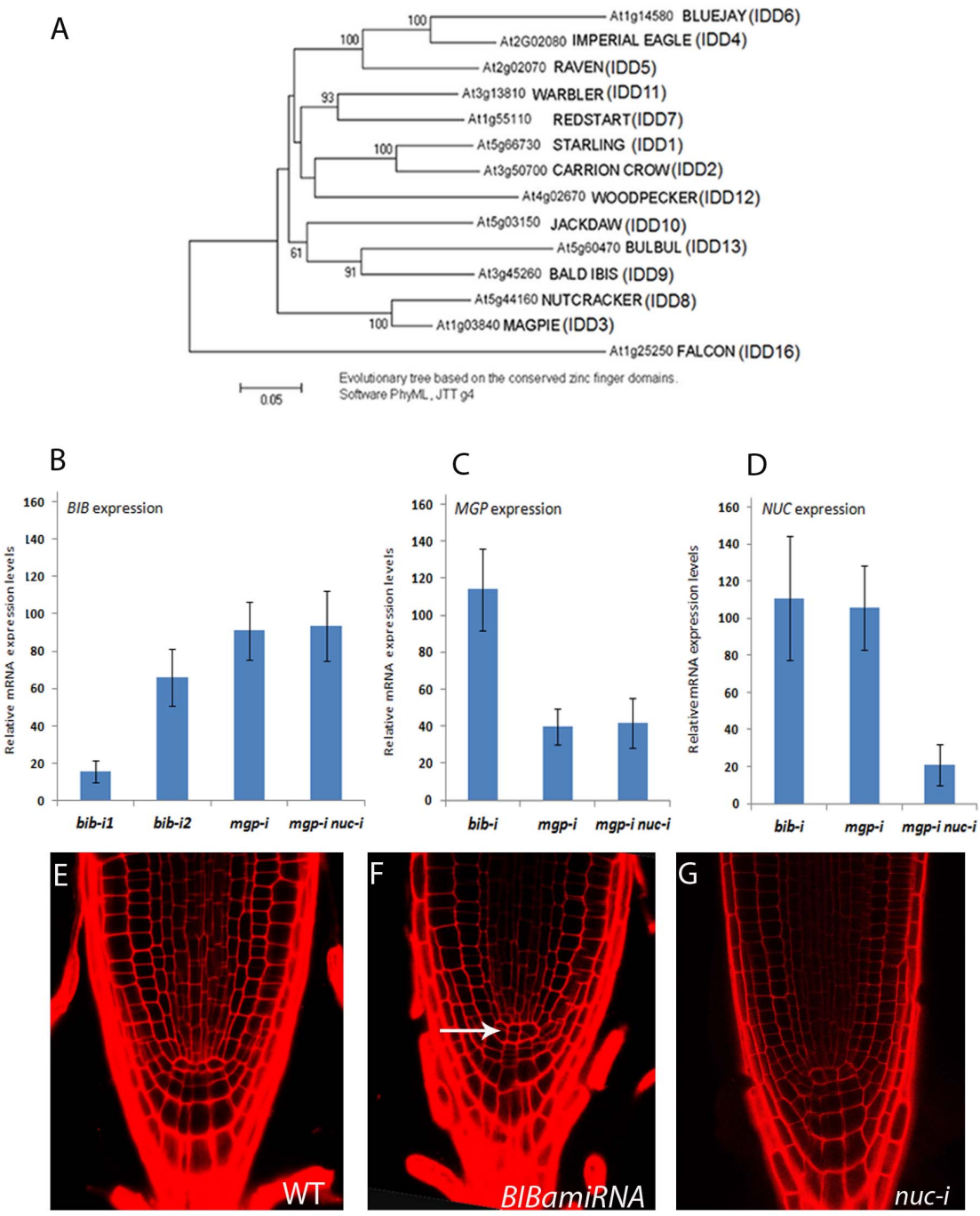

Supplemental Figure 1. Phylogenetic analysis of BIRD protein sequences and transcript levels in BIRD RNAi lines relative to that in WT determined by RT-qPCR.

A. Phylogenetic analysis of BIRD proteins (also known as IDD proteins) based on their conserved zinc finger domains, Statistical support to assess the significance of phylogenetic grouping was evaluated using 100 bootstrap replicates. Numbers on the nodes show the statistical support of values above 50%.

B-D Transcripts levels of *BIB* (B), *MGP* (C) and *NUC* (D). For *BIB*, RNA levels were determined in two independent *BIB* RNAi lines (*bib-i1* and *bib-i2*), *mgp-i* and *mgp-i nuc-i. MGP* and *NUC* expression levels were also determined in *bib-i*, *mgp-i* and *mgp-i nuc-i*. Relative mRNA levels were determined by quantitative real time PCR represented as percentages. Numbers on y-axes are in percentage, error bars represent standard deviations. Each experiment was repeated for three biological replicates.

E-G Median longitudinal confocal sections of 7 days old roots of WT (D), *BlBamiRNA* (E) and *nuc-i* (G). Arrow indicates abnormal divisions occurring in the QC.

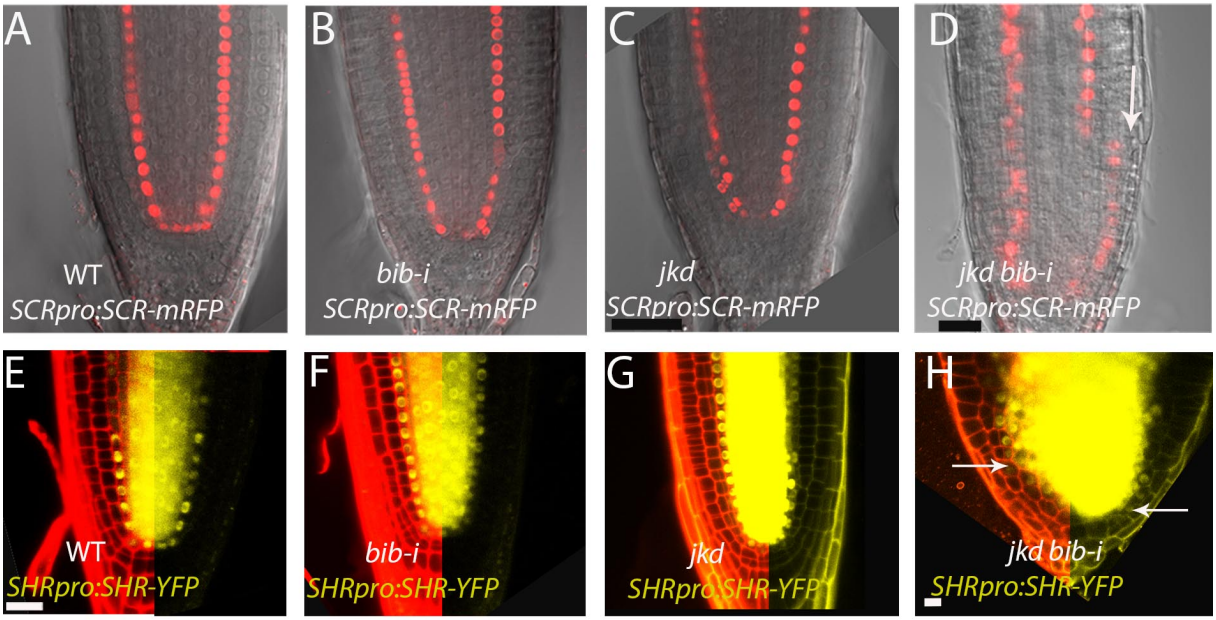

Supplemental Figure 2: Outward Shift in SCR expression domain *in jkd bib-i* correlates with SHR spread.

A-D Confocal images showing 7 days old roots expressing *SCRpro:SCR-mRFP* in WT (A), *bib-i* (B), *jkd* (C) and *jkd bib-i* (D), arrow points to expression of SCR-mRFP in the epidermis in *jkd bib-i* (D). Scale bars represent 20 µm.

E-H Confocal images of 7 days old roots expressing *SHRpro:SHR-YFP* of WT (E), *bib-i* (F), *jkd* (G) and *jkd bib-i* (H). Scale bars are 20 µm

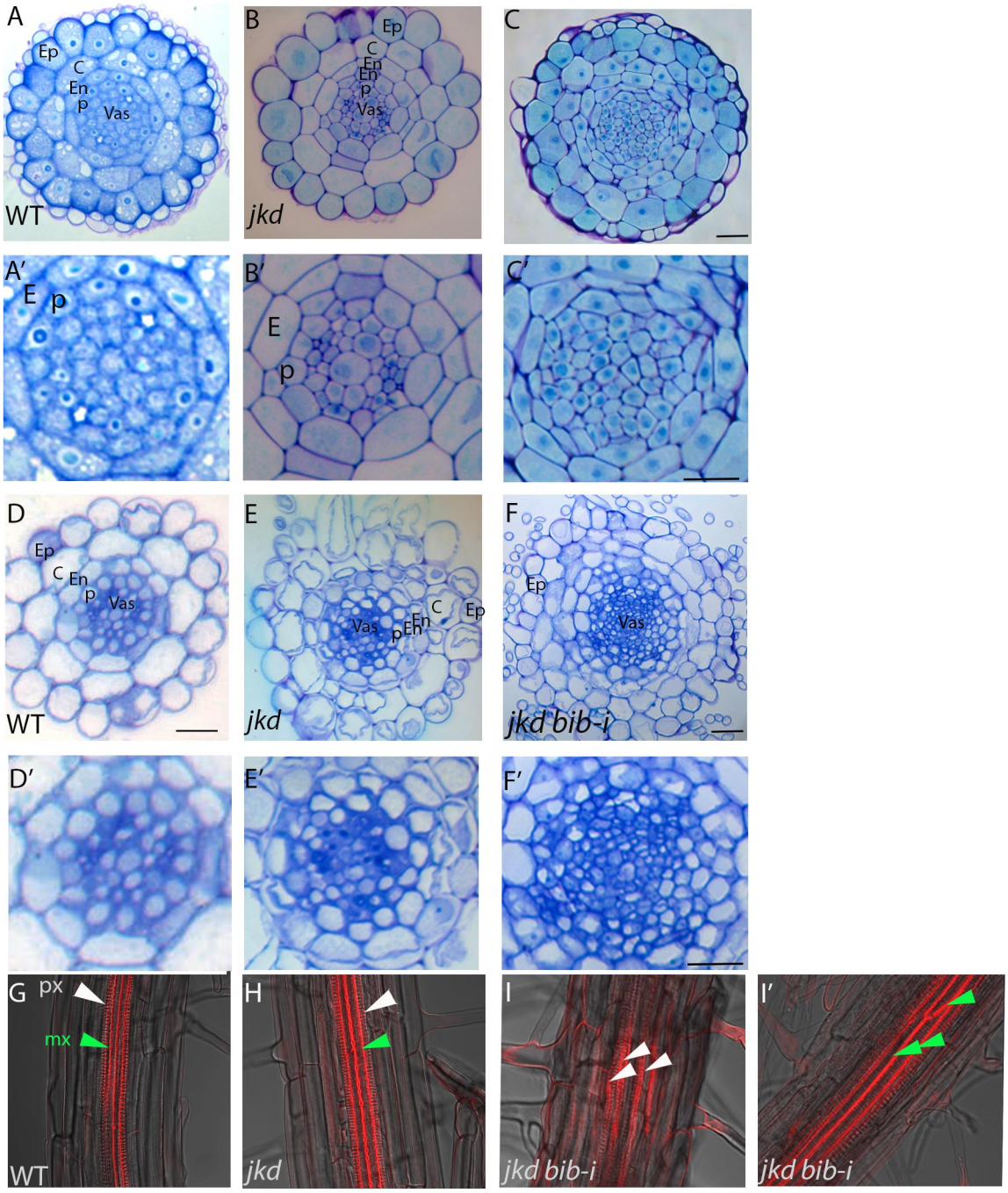

Supplemental Figure 3. Increased cell number of vasculature in *jkd bib-i*.

A-F' Toluidine blue images of stained cross sections taken from different zones of 5 days old roots of WT (A, A'; D, D''), *jkd* (B, B'; E, E'), *jkd bib-i* (C, C'; F, F'). A-C: Sections are from the meristematic region. D-F: Sections are at the differentiation zone. A', B', C', D', E' and F' are enlarged images from A, B, C, D, E and F. Note the increase in cell number of the vascular bundle in F and F''. Scale bar represents 50 µm

A and C are the same images of roots sections in Figure 2 O and P. Ep: epidermis, C: cortex, En: endodermis; vas: vasculature, P: pericycle. G-I' Confocal images of fuchsin-stained xylem in roots of WT (G), *jkd* (H) and *jkd bib-i* (I, I'). Note increased number of protoxylem (white arrowheads in I) and metaxylem (green arrowheads in I').

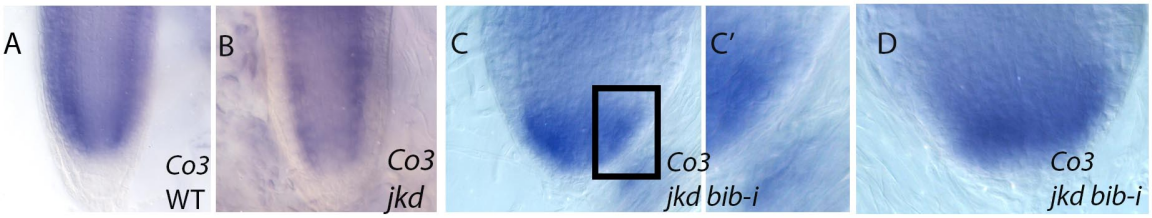

Supplemental Figure 4. JKD and BIB constrain cortex marker to one single layer
A-D Whole mount in situ hybridization using a cortex specific gene Co3 in 7 days old roots of WT (A), *jkd* (B), *jkd bib-i* (C-D). Note expansion of cortex marker inwards and outwards the radial axis *in jkd bib-i*.

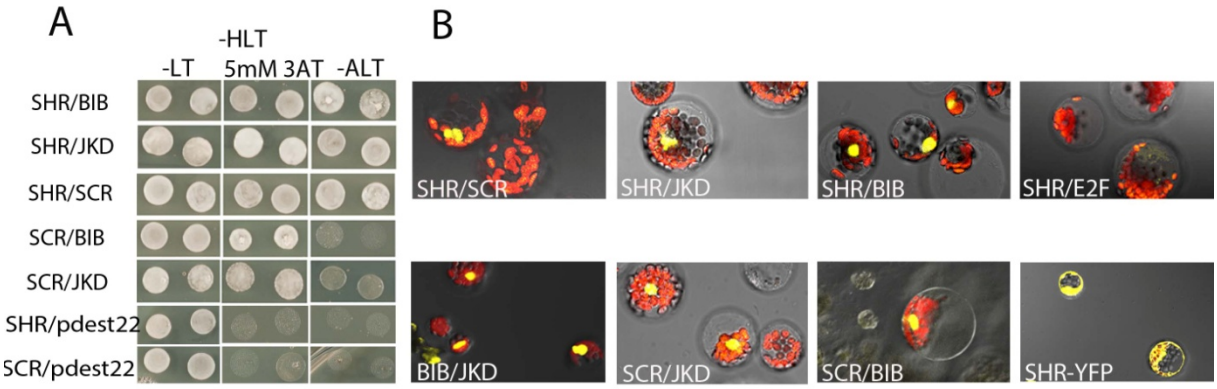

Supplemental Figure 5. BIB and JKD proteins interact with SCR, SHR and among themselves.

A Yeast two-hybrid assay determining interactions by growth rates on selective medium His-Leu-Trp-(-HLT) supplemented with 5mM of 3-Amino-1,2,4-triazole (3-AT) and Ala- Leu-Trp- (-ALT). BIRD proteins were used as prey while SCR and a non-autoactivating form of SHR were used as bait. The SCR and SHR pair was used as a positive control while SCR/pdest22 and SHR/pdest22 pairs were used as negative controls.

B Bimolecular fluorescence complementation assay in protoplasts reveals that BIRD proteins interact with SCR, SHR and themselves. The SHR/SCR pair was used as a positive control, SHR/E2F pair was used as a negative control. Note that SHR-SYFP showing nuclear and cytoplasmic localization.

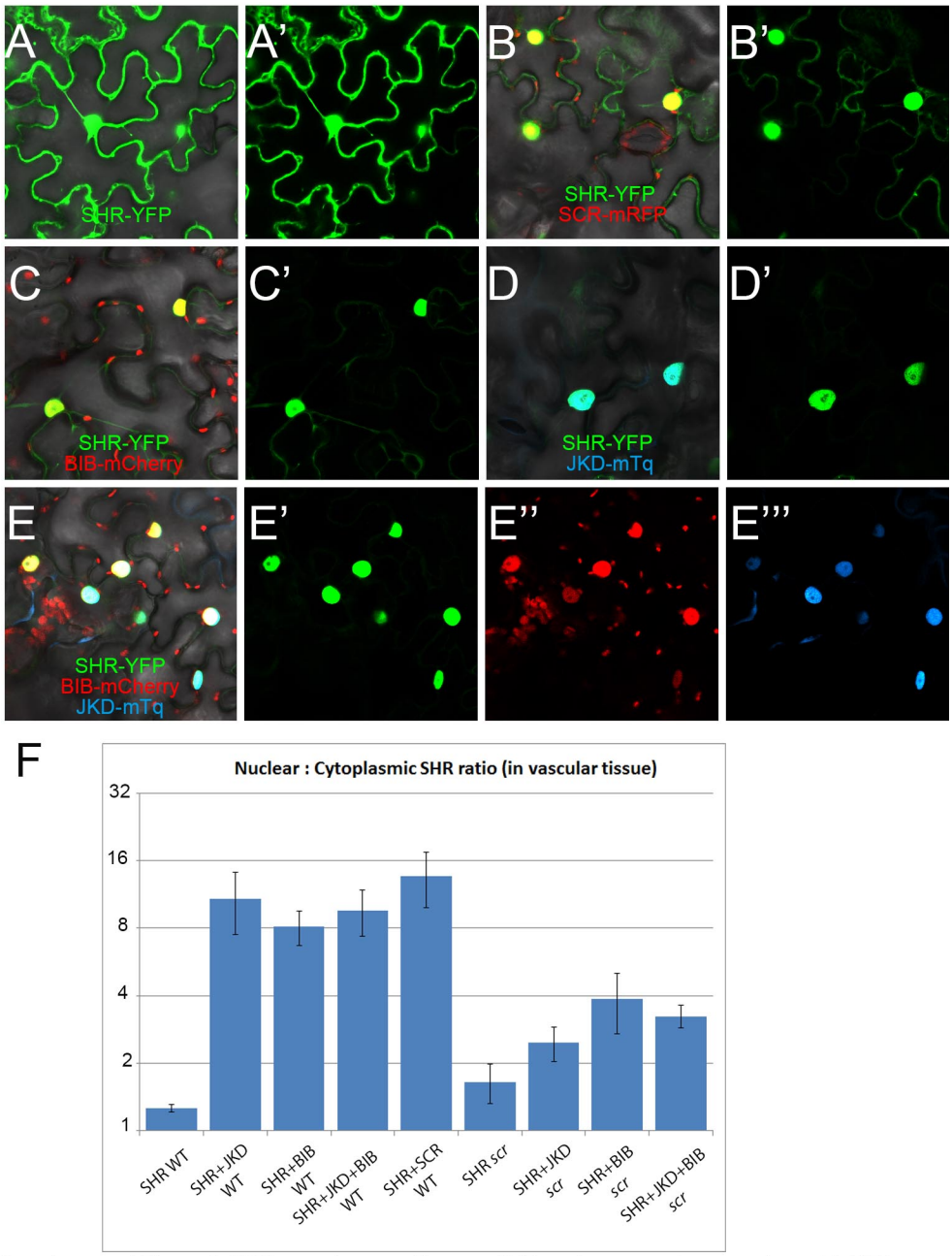

Supplemental Figure 6. BIRD proteins contribute to SHR nuclear retention together with SCR.

A-E''' Transient expression assays in *Nicotiana bentamiana* leaf epidermal cell of SHR-YFP (A, A'), SHR-YFP in presence of SCR-mRFP (B,B'), BIB-mcherry (C,C'); JKD-mTq(D,D') and BIB-mcherry + JKD-mTq (E, E"').

F Quantification of nuclear and cytoplasmic fluorescence signal in plant expressing BIRDs and SCR in vascular tissue in presence and absence of SCR. Error bars in F represent standard error of mean (SEM).

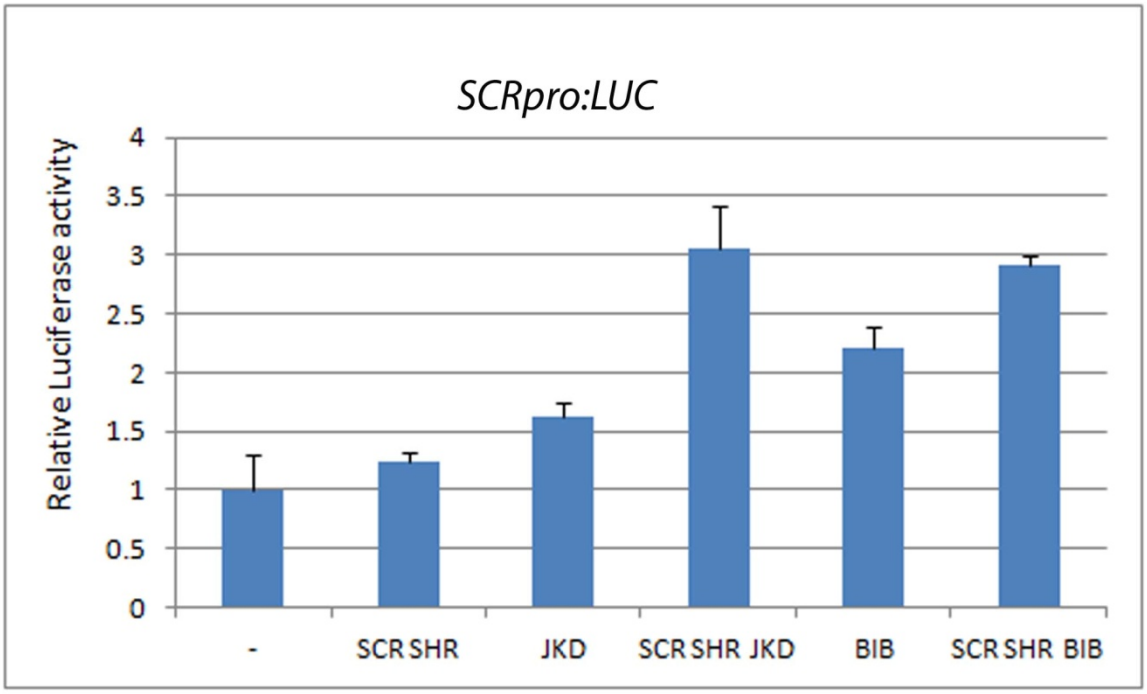

Supplemental Figure 7. JKD and BIB activate *SCR* expression more efficiently than SCR-SHR complex.

Promoter activity measured by Dual Luciferase assay using protoplasts transiently co-transformed with firefly luciferase under *SCR* promoter and effectors plasmids carrying SCR, SHR, BIB or JKD driven by CaMV 35S promoter. BIB and JKD induce *SCR* promoter activity independently from SCR-SHR complex.

Error bars represent standard error of mean (SEM). Each experiment was repeated at least three times with three technical and three biological replicates.

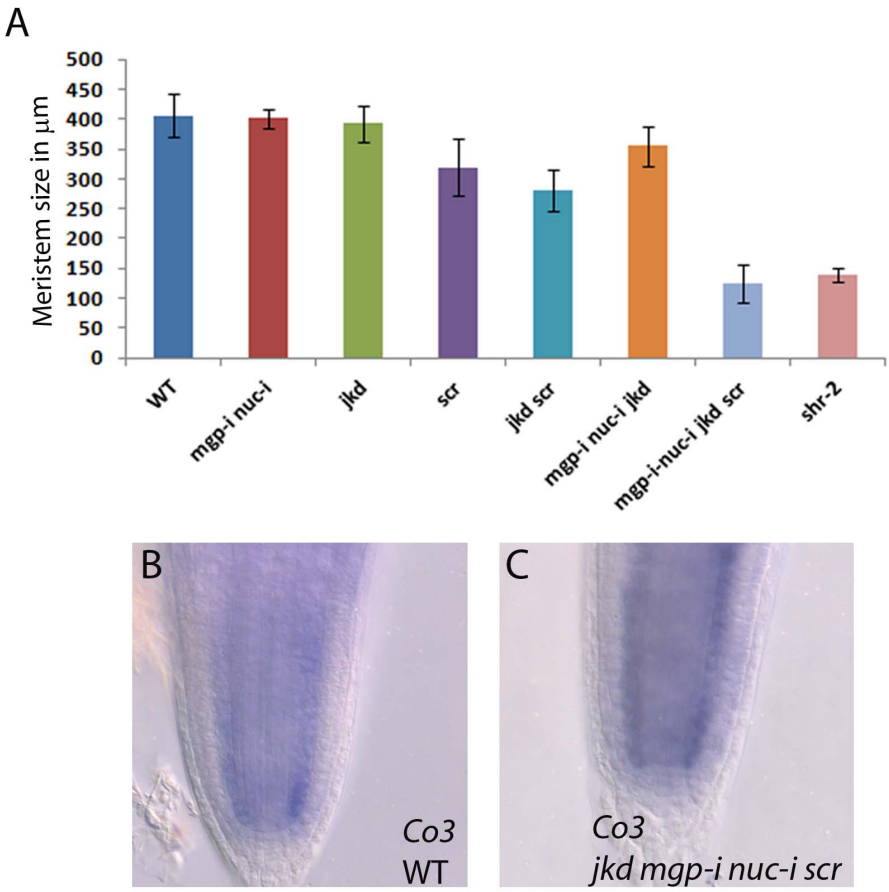

Supplemental Figure 8. *JKD, MGP, NUC* and *SCR* genes control root meristem size but do not influence cortex cell fate.

A *jkd mgp-i nuc-i scr* roots display a reduction of meristem size similar to the one observed in *shr*. Y-axis represents the meristem size in µm. Error bars represent standard deviations. For each line the meristems of at least 20 plants were measured.

B, C Whole mount *in situ* hybridization using a cortex-specific gene *Co3* in 3 days old roots of WT (B) and *jkd mgp-i nuc-i scr* (C).

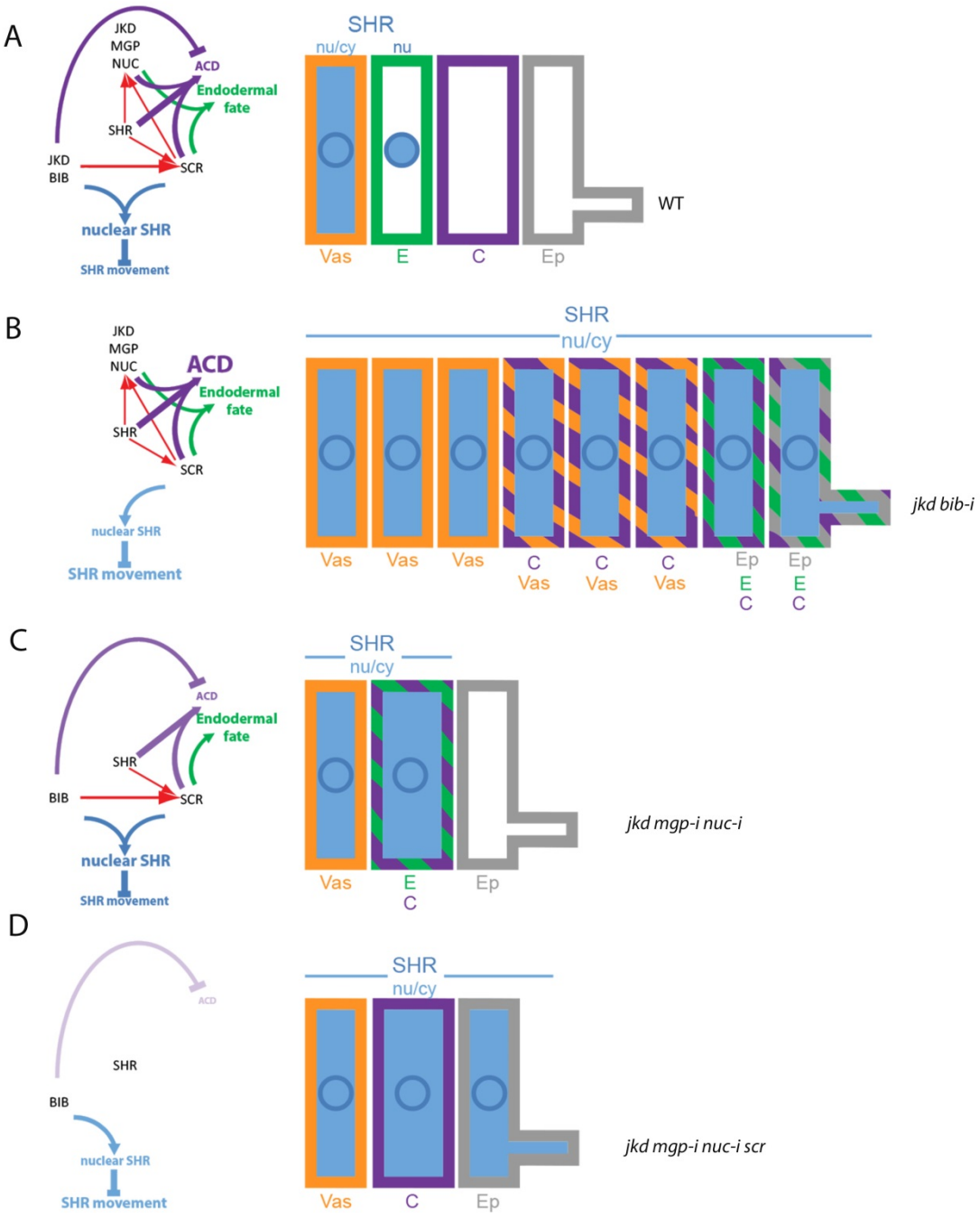

Supplemental Figure 9. Model illustrating BIRD action on SHR movement range and root radial pattern specification.

A In WT, JKD, BIB and SCR promote SHR nuclear retention (thick blue arrow) and restrict SHR movement (thick inhibition sign) in part through *SCR* activation (red arrow) which in turn together with SHR promotes *JKD*, *NUC* and *MGP* expression. All together they contribute to asymmetric cell division (thick purple arrow) and endodermal fate specification (thick green arrow). JKD and BIB restrict ACD and promote normal boundaries specification leading to one layer from each tissue.

B In *jkd bib-i,* SHR spread is accompanied by excessive divisions leading to loss of tissue boundaries.

C In *jkd mgp-i nuc-i,* ACD in ground tissue is restricted but endodemal fate is still maintained.

D In *jkd mgp-i nuc-i scr,* excessive SHR movement is not sufficient to trigger ACD and endodemal fate requires activity of the four proteins.

Supplemental Tables

Primers	Forward	Reverse
EcoRI-SHR-BamHI	CCGGAATTCATGGATACTCTCTTTAGAC	CGCGGATCCGCCGTTGGCCGCCACGC
KpnI-SCR-AgeI	CGGAATTCATGGATACTCTCTTTAGAC	CGCGGATCCGCCGTTGGCCGCCACGC
AfeI-JKD-AgeI	GCTAGCGCTATGCAGATGATTCCAGG	GCGACCGGTATACCCAATGGAGCAAACC
mCherry-BIB	GGAATTCCATGATGATGCCAGATGATC	GACGTCGACTTACTGGTTCATGTCGGCGG

Supplemental Table 1: primers used to generate Constructs for transformation in Hela cells

Constructs	Reference
SHR-YFP	This study
JKD-mCherry	This Study
mCherry-BIB	This Study
SCR-mTurquoise	This Study

Supplemental Table 2: Constructs used for Hela cells transformation

Construct	Vector	Reference
SHR-YFP	pB7m34GW	This Study
JKD-mCherry	pH7m34GW	This Study
SCR-mRFP	pH7m34GW	This Study
BIB-CFP	pH7m34GW	This Study
CYCD6pro:LUC	pUWG35	This Study
SCRpro:LUC	pUWG35	This Study

Supplemental Table 3: Effectors and promoter constructs used for Luciferase activity in protoplasts

Primer name	Forward	Reverse
qPCR MGP	CGCTCTCTTTATGGTCGGGAGG	CGGAAAGAGAAGTTGCCCCGTTAGCG
qPCR NUC	CAACCATTTGTACCACAACCGC	GGGGCAGAGAGAGTAGTGGTAGTGG
qPCR BIB	CAAGCTCAAGCAATAGCAAGAC	GTGGAGGCCGGAGGAGACGAGTCTGG
qPCR ACTIN	GGCGAAGATGTGGCAGAGCA	ACGAGGATTCGGTGCAGGACCT
SCRpro	CCGATTGAGAGGAGAGGATTGACCGG	AGATTGCATGGTTATAAATAAGGT
CYCD6pro	CTCTGCAAGTGCAGAAACAAAGTACATTTTAG	TGGTGTTAGAAGATGAAGAAGAAG
Attsites pDNR221	GGGGACAAGTTTGTACAAAAAAGCAGGCTG	GGGGACCACTTTGTACAAGAAAGCTGGGTT
SHRpro 2.5KB	TTTCGAGAAATTACATAAGAAACTGAATT	TAAATCTTAGATATTGTGGGTCTTAC
NUCpro 2,6kb	CTCTCTTTATTAGTTTAGGAAG	GAGAGAGAGAGAGAGAGAAGGAGAC
BIBpro	ATTSITES-GAGTCTCTTTGACAACAGACATCTGGA	ATT-SITESTCCCACAAGACTTATAGAGAAGTAAGCAC
att sites	GGGGACAACTTTGTATAGAAAA	GGGGACTGCTTTTTTGTACAAACTTG

pGMETeasy1R4	GTTGCG	C
NUC cds	ATGACAAGTGAAGTTCTTCAAAC AATCTCAAGTGG	AATCCATCCATTGATAGACGATGGAT GGCAC
BIB cds	ATGATGATGCCAGATGATCATCA	CTGGTTCATGTCGGCGGTTGGTGTG CCG
Co3 probe	CACTGTCTGGCCTGGGATC	TCGCAATGCTAGTTGGGTC

Supplemental Table 4: Primers sequences used in this study

Lines	Plant vector	Plant Resistance	Reference
SCRpro:SCR-YFP	pB7m34GW	ppt	Cruz Ramirez et al., 2012
SHRpro:SHR-vYFP	pGreenII0029	ppt	This study
JKDpro:JKD-YFP	pB7m34GW	ppt	This study
JKDpro:HIS2B-YFP	pGreenII0025	norf	This study
BIBpro:BIB-YFP	pB7m34GW	ppt	This study
BIBpro:HIS2B-YFP	pGreenII0025	norf	This study
NUCpro:NUC-YFP	pB7m34GW	ppt	This study
MGPpro:MGP-GFP	pGreenII0029	ppt	Cruz ramirez et al., 2012
SCRpro:SCR-mRFP	pH7m34GW	hyg	This study
WOLpro:SCR-mRFP	pH7m34GW	hyg	This study
WOLpro:XVE>>JKD-mcherry	pH7m34GW	hyg	This study
WOLpro:XVE>>BIB-CFP	pH7m34GW	hyg	This study
CYCD6pro:GFP	pKGWFS7-Dx	ppt	Sozzani et al., 2010
bib-i	pAGRIKOLA	ppt	This study
mgp-i	pGreenII0025	MTX	Welch et al., 2007
nuc-i	pHellsgate	Kan	This study

Supplemental Table 5: Transgenic lines used in this study

Supplemental methods

Phylogenetic analysis

The 13 protein sequences from the Arabidopsis members of the Zinc finger protein family A1a and one member of A1b (At1g25250), described in Englbrecht et al., 2004, were aligned using Muscle (Edgar et al., 2004) and careful manual adjustment of the alignment to remove unambiguously positions was done using Bioedit (Hall et al., 1999). Based on the final multiple sequence alignment containing 233 sites, a phylogenetic tree was constructed using maximum likelihood in PhyML (Guidon et al., 2003) using as model for amino acids substitution JTT with a discrete gamma distribution (4 categories). Statistical support to assess the significance of phylogenetic grouping was evaluated using 100 bootstrap replicates. The final unrooted tree was generated using MEGA Tree Explorer (Tamura et al., 2011).

References

Englbrecht CC, Schoof H, Böhm S. Conservation, diversification and expansion of C2H2 zinc finger proteins in the Arabidopsis thaliana genome. BMC Genomics. 2004; 5(1):39

Edgar RC: MUSCLE: a multiple sequence alignment method with reduced time and space complexity. BMC Bioinformatics, 2004; 5:113.

Hall TA: BioEdit: a user-friendly biological sequence alignment editor and analysis program for Windows 95/98/NT. Nucleic Acids Symposium Series, 1999; 41:95-98

Guindon S, Gascuel O: A simple, fast, and accurate algorithm to estimate large phylogenies by maximum likelihood. Syst Biol 2003; 52(5):696-704.

Tamura K, Peterson D, Peterson N, Stecher G, Nei M, and Kumar S. MEGA5: Molecular Evolutionary Genetics Analysis using Maximum Likelihood, Evolutionary Distance, and Maximum Parsimony Methods. Molecular Biology and Evolution. 2011; 28: 2731-2739.